Development and Evaluation of One-Dimensional Model for Annular UV-H_2O_2 Photoreactors

Mostafa Moghaddami, Mehrdad Raisee, and Alireza Jalali

***Abstract*—To use wastewater for aggregating vast farm lands it is necessary to disinfect harmful pollutants in the wastewater. UV-H_2O_2 photoreactors are capable of degrading the recalcitrant pollutants and other conventional pollutants. The simulation of the reactor prior to its manufacturing can help the designer to obtain the main parameters of the reactor to meet the best disinfection performance of the reactor and the least energy consumption. Many researchers used one-dimensional models to predict the performance of the UV-H_2O_2 photoreactor. In this paper a simplified one-dimensional model for an annular UV-H_2O_2 reactor is presented and its performance is compared with a 2D model. In this one-dimensional model a plug like velocity profile is assumed for the wastewater flow and the point source summation (PSS) model is used to obtain the UV radiation field. The accuracy of the one-dimensional model is compared with the validated two-dimensional model. Obtained results show that in the investigated annular reactor the error of one dimensional model for hydroxyl radical is about 50% and the error of contaminant removal is about 10%.**

***Index Terms*—UV-H_2O_2 photoreactors, one-dimensional model, annular reactor.**

I. Introduction

The enormous diversity of toxic and emerging pollutant components (such as persistent organic pollutants (POPs), endocrine disruptors, and pharmaceutically active agents) suggests that no universal treatment method can be advanced thus leading to the development of contaminant-specific decontamination processes. Among the most promising emerging chemical oxidation processes, Advanced Oxidation Processes (AOPs) have provided innovative, often cost-effective, catalyzed chemical oxidation for treating pollutants in low or high concentration from contaminated soil, sludge and water.

Advanced Oxidation Processes, refers to a set of chemical treatment procedures designed to remove organic and inorganic materials from water by oxidation. AOPs are particularly useful for treating biologically refractory compounds which are converted to a large extent into stable inorganic compounds such as water, carbon dioxide and salts.

Production of hydroxyl radicals can be initiated by direct photolysis of hydrogen peroxide (H_2O_2) under UV irradiation. The detailed and validated mechanism of this process has been reported in previous studies. Stefan et al.[1] conducted an investigation to study the kinetics and mechanism of acetone degradation in dilute aqueous solution, sensitized by UV-H_2O_2 photolysis, with the aim of explaining why its treatment is slow. The roles of some parameters, such as the pH and the initial concentrations of acetone and H_2O_2, were examined in order to provide a full description of the system. The proposed kinetic model produced profiles for reactants and intermediates which were in agreement with the experimental data. Later Crittenden et al.[2] proposed a dynamic kinetic model for the advanced oxidation process (AdOx) using hydrogen per-oxide and ultraviolet irradiation (H_2O_2/UV) in a completely mixed batch reactor (CMBR). Literature reported photochemical parameters and chemical reaction rate constants were used in their model to describe the kinetic rates of all the main species in the solution, and to predict the organic compound destruction giving reliable predictions of the destruction of the target organic compounds.

For accurate prediction of a UV-H_2O_2 AOP performance it is also crucial to accurately predict spatial distribution of irradiance correctly. Bolton [3] described the optics of cylindrical UV reactors in detail and presented a sophisticated model that accounts for reflection and refraction as a beam of UV radiation passes through an air/quartz/water interface. Liu et al.[4] performed a detailed investigation to examine the performance of various radiation models. The models tested were line source integration (LSI), point source summation (PSS), multiple segment source summation (MSSS), UVCalc3D (a commercial software based on MSSS), RAD-LSI (modified version of LSI) , and discrete ordinate (DO) of Fluent CFD software. The fluence rates obtained with these models were compared with irradiation measurements for air and water. Their results clearly indicated that the effects of refraction must be taken into consideration for accurate prediction of fluence rate distribution. Sasges et al.[5] described the shortcomings of the Point Source Summation (PSS) model and showed the development of a Lambertian model.

Several researchers have used CFD for analyzing and improving the hydraulics through UV systems. Machairas [6] investigated how application of an annular UV/H_2O_2 reactor can remove three phosphate esters from drinking water. Phosphate esters considered were: tributyl phosphate (TBP), tri(2-chloroethyl) phosphate (TCEP), and tri(2-butoxyethyl) phosphate (TBEP). A simple cylindrical rector was considered. The lamp in the UV reactor was modeled a line source and then approximated as a series of point sources (PSS model). A plug like uniform velocity profile was assumed and the conservation of mass of various species in Lagrangian framework were solved using MATLAB software. Their results indicated that TBEP is degraded the most among three target phosphate esters.

Manuscript received May 25, 2012; revised July 8, 2012.

M. Moghaddami and M. Raisee are with School of Mechanical Engineering, College of Engineering, University of Tehran, Tehran, Iran (e-mail: moghaddamy@yahoo.com; mraisee@ut.ac.ir).

A. Jalali is with Department of Mechanical Engineering, University of British Columbia, 2324 Main Mall, Vancouver, BC V6T 1Z4, Canada.

It is well known that the performance of ultraviolet (UV) reactors used for water treatment is greatly influenced by the reactor hydrodynamics. Sozzi and Taghipur [7] numerically investigated turbulent flow through complex L-shape and U-shape UV-reactor configurations using Fluent software. They compared velocity vectors and velocity profiles with the results obtained from particle image velocimetry (PIV) experiments ([7]). They examined the influence of mesh structure and density, as well as the effectiveness of three different turbulence models namely: Standard $k-\varepsilon$, Realizable $k-\varepsilon$, and Reynolds stress model (RSM), on the simulation results. They found that the Realizable $k-\varepsilon$ displays the best overall match to the experimental PIV measurements. Liu et al.[8] employed six turbulence models, including variants of $k-\varepsilon$, $k-\omega$ turbulence models, Reynolds stress transport model (RSTM), and two-fluid model (TFM) to simulate a polychromatic UV reactor. Their results showed that the irradiation distributions and the effluent inactivation levels are sensitive to the turbulence model. The level of sensitivity was a function of the operating conditions and the UV response kinetics of the microorganisms. A broader fluence distribution was found with turbulence models that predicted a larger wake region behind the lamps. Shao [9] and Hofman et al.[10] performed computations for a cylindrical UV reactor with three different lamp configurations and two different flow rates of $2m^3/h$ and $5m^3/h$. Among three lamp configurations examined, staggered lamp arrangement gave the highest average UV dose as well as the narrowest dose distribution pattern. Model also predicted low pressure lamps have about 8% higher power output to UV dose efficiency than medium pressure lamps. The $k-\varepsilon$ turbulence model produced generally good qualitative prediction of flow inside the reactor but failed to give correct prediction of recirculation zones behind the quartz tubes.

Limited studies have been devoted to CFD simulation of UV/AOPs reactors. Pareek et al.[11] used CFD combined with a discrete-ordinate radiation transport equation for UV intensity and modified $k-\varepsilon$ turbulence equations to model a heterogeneous, multi-phase photocatalytic reactor system for the photodegradation of contaminants. However, the applied radiation model did not incorporate refraction and was used to describe a simple bench scale reactor. More recently, Santoro et al.[12] developed a comprehensive kinetic model of UV-H_2O_2 AOP that was coupled with the Reynolds averaged Navier-Stokes (RANS) equations. They used CFD to predict the oxidation of tributyl phosphate (TBP) and tri (2- chloroethtyl) phosphate (TCEP) in two different photo-reactors: a parallel- and a cross-flow UV device. CFD simulations obtained for both turbulent and laminar flow regimes and compared with experimental data over a wide range of UV doses. Although two-dimensional CFD models provide more accurate data about the species distributions in the reactor, it is computationally expensive and simpler 1D model is expected more efficient for engineering design of photo reactors.

In the current paper, a one-dimensional model has been developed and evaluated to predict the chemical and physical state of an annular UV-H_2O_2 photo-reactor. The results of the developed 1D model are compared with the results of the 2D model presented in Santoro et al.[12]. Although solving the two-dimensional governing equations of fluid dynamics and fluence rate gives a more accurate estimation of properties, 1D simulation may be accurate enough for the simulation.

II. Methods

A. Governing Equations of 1D Simulation

To simulate the annular photoreactor it is assumed that the velocity profile is uniform, and the mass species equation can be simplified as equation

$$\frac{\partial Y_i}{\partial t} = R_i \tag{1}$$

The index "i" represent for each chemical species in the simulation. The kinetic model was incorporated into CFD using numerical subroutines to prescribe the net rate of generation, Ri, for each chemical species considered.

$$\begin{aligned} R_{H_2O_2} &= -2.303\phi_{H_2O_2} I(\varepsilon_{H_2O_2}[H_2O_2] + \varepsilon_{HO_2^-}[HO_2^-]) \\ &-k_2[H_2O_2][OH\bullet] - k_3[HO_2^-][OH\bullet] \\ &-k_4[H_2O_2][HO_2\bullet] - k_5[H_2O_2][O_2^-\bullet] \\ &-k_8[H_2O_2][CO_3^-\bullet] - k_9[HO_2^-][CO_3^-\bullet] + k_{10}[OH\bullet][OH\bullet] \\ &+k_{12}[HO_2\bullet][HO_2\bullet] + k_{13}[HO_2\bullet][O_2^-\bullet] \end{aligned} \tag{2}$$

$$\begin{aligned} R_{OH\bullet} &= 2\times 2.303\phi_{H_2O_2} I(\varepsilon_{H_2O_2}[H_2O_2] + \varepsilon_{HO_2^-}[HO_2^-]) \\ &-k_2[H_2O_2][OH\bullet] - k_3[HO_2^-][OH\bullet] \\ &+k_4[H_2O_2][HO_2\bullet] + k_5[H_2O_2][O_2^-\bullet] \\ &-k_6[OH\bullet][CO_3^{2-}] - k_7[OH\bullet][HCO_3^-] \\ &-2k_{10}[OH\bullet][OH\bullet] - k_{11}[OH\bullet][HO_2\bullet] \\ &-k_{14}[OH\bullet][O_2^-\bullet] - k_{15}[OH\bullet][CO_3^-\bullet] \\ &-k_{TBP}[OH\bullet][TBP] - k_{TCEP}[OH\bullet][TCEP] \\ &-k_{TBEP}[OH\bullet][TBEP] \end{aligned} \tag{3}$$

$$\begin{aligned} R_{CO_3^-\bullet} &= k_6[OH\bullet][CO_3^{2-}] + k_7[OH\bullet][HCO_3^-] \\ &-k_8[H_2O_2][CO_3^-\bullet] - k_9[HO_2^-][CO_3^-\bullet] \\ &-k_{15}[OH\bullet][CO_3^-\bullet] - k_{16}[O_2^-\bullet][CO_3^-\bullet] \\ &-2k_{17}[CO_3^-\bullet][CO_3^-\bullet] \end{aligned} \tag{4}$$

$$\begin{aligned} R_{HCO_3^-} &= -k_6[OH\bullet][CO_3^{2-}] - k_7[OH\bullet][HCO_3^-] \\ &+k_8[H_2O_2][CO_3^-\bullet] + k_9[HO_2^-][CO_3^-\bullet] \\ &+k_{16}[O_2^-\bullet][CO_3^-\bullet] \end{aligned} \tag{5}$$

$$\begin{aligned} R_{O_2^-\bullet} &= k_2[H_2O_2][OH\bullet] + k_3[HO_2^-][OH\bullet] \\ &-k_4[H_2O_2][HO_2\bullet] - k_5[H_2O_2][O_2^-\bullet] \\ &+k_8[H_2O_2][CO_3^-\bullet] + k_9[HO_2^-][CO_3^-\bullet] \\ &-k_{11}[OH\bullet][HO_2\bullet] - 2k_{12}[HO_2\bullet][HO_2\bullet] \\ &-k_{13}[HO_2\bullet][O_2^-\bullet] - k_{14}[OH\bullet][O_2^-\bullet] \\ &-k_{16}[O_2^-\bullet][CO_3^-\bullet] \end{aligned} \tag{6}$$

$$R_{TBP} = -k_{TBP}[OH\bullet][TBP]$$
$$R_{TCEP} = -k_{TCEP}[OH\bullet][TCEP] \quad (7)$$
$$R_{TBEP} = -k_{TBEP}[OH\bullet][TBEP]$$

The *k* factors are rate constants and their values could be found in [12].

At near-neutral pH, the concentrations of species such as $HO_2?$, HO_2^- and CO_3^{2-} are negligible if compared to those of their conjugate acid/base $O_2^-?$, H_2O_2 and HCO_3^-. For a buffered system, they can be estimated as follows:

$$[CO_3^{2-}] = \frac{10^{-10.3}[HCO_3^-]}{[H^+]} \quad (8)$$

$$[HO_2^-] = \frac{10^{-11.6}[H_2O_2]}{[H^+]} \quad (9)$$

$$[HO_2\bullet] = \frac{[H^+][O_2^-\bullet]}{10^{-4.8}} \quad (10)$$

To evaluate the incident radiation in the UV-H_2O_2 photoreactor the point source summation model is used. In this model the UV lamp is modeled as a set of small spherical elements. Fig. 1 displays division of the UV lamps into spherical elements. The incident radiation in the UV-H_2O_2 photoreactor is calculated by assuming the total effects of all spherical point source elements.

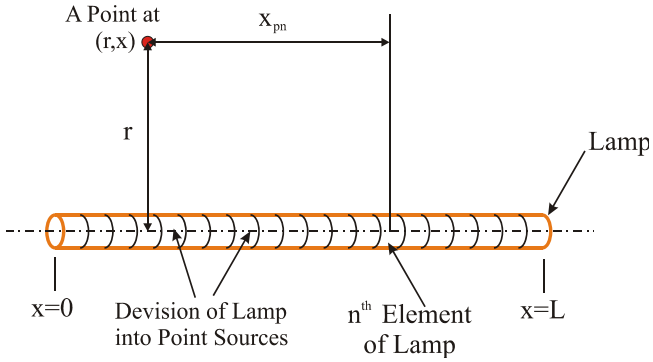

Fig. 1. Configuration of Point source elements on the UV lamp.

The total incident radiation in each point can be calculated by the following equation.

$$I(r,x) = \sum_{n=1}^{n=N}\left(\frac{P/N}{4\pi(r^2+x_{pn}{}^2)}e^{-a\sqrt{r^2+x_{pn}{}^2}}\right) \quad (11)$$

where P is the UV lamp power, n is the number of each point source element, N is the total number of point source elements on the lamp, r is the distance between the point and lamp axis, *a* is the absorption coefficient of the fluid and xpn is the distance between the each element and the point at (r,x) coordinate. xpn is calculated by the following equation:

$$x_{pn} = x - n(L/N) \quad (12)$$

where L is the length of the UV lamp.

B. Governing Equations of 2D Simulation

The numerical predictions of 2D simulation were carried out using the Fluent 6.3 software. The governing equations in two dimensional simulations are shown in equations 1-3. All the flow and mass transfer equations are presented in Cartesian tensor notation. For a steady incompressible flow, the conservation laws of mass, momentum and concentration are written as:

Continuity:

$$\frac{\partial U_j}{\partial x_j} = 0 \quad (13)$$

Momentum:

$$\frac{\partial (U_j U_i)}{\partial x_j} = \frac{-1}{\rho}\frac{\partial P}{\partial x_i} + \frac{\partial}{\partial x_j}\left(\nu\frac{\partial U_i}{\partial x_j} - \overline{u_i u_j}\right) \quad (14)$$

Mass species:

$$\frac{\partial (U_j Y_i)}{\partial x_j} = \frac{\partial}{\partial x_j}\left(\frac{\nu}{Sc}\frac{\partial Y_i}{\partial x_j} - \overline{u_j y_i}\right) + R_i \quad (15)$$

where ρ, ν and *Sc* are respectively, the density, the kinematic viscosity and the Schmidt number.

In equation (3), R_i represents the net rate of production by chemical reaction for each component included in the CFD model.

In the 2D model, the standard high-Re *k-ε* model was used to describe turbulent flows in annular reactor. Such choice is justified by the extreme simplicity of the flow field in an annular reactor, where the standard high-Re *k-ε* model is expected to provide reasonable results.

The calculation of the fluence rate field was carried out by solving the radiation transport equation (RTE) using the discrete ordinate model ([13]). In the discrete ordinate (DO) model, the RTE is solved for the spectral intensity $I_\lambda(\vec{r},\vec{s})$:

$$\nabla.\left(I_\lambda(\vec{r},\vec{s}),\vec{s}\right) + a_\lambda I_\lambda(\vec{r},\vec{s}) = 0 \quad (16)$$

where $\vec{r}$ and $\vec{s}$ are position and direction vectors respectively, λ is the wavelength and a_λ is the spectral, spatially-dependent fluid absorption coefficient.

C. Geometry

An annular UV-H_2O_2 photoreactor, considered in this paper consists of a UV lamp with 4 cm diameter and a cylindrical quartz sleeve that covers the UV lamp and prevent the direct contact of water and the UV lamp. Fig. 2 displays the cross section view of the annular reactor. In the 2D simulations both air and water regions are simulated precisely but in the 1D model only the water region is modeled. The inner radius of the annular reactor is 2.5 cm and the outer radius in different cases is 5, 10, 20 and 40 cm. The inlet velocity of the water is assumed to be 0.1 m/s and the Reynolds number of the wastewater flow in the annular photoreactor is between 250000 to 3750000. It is assumed that the wastewater is a buffered with constant pH of 7. At the inlet of UV-H_2O_2 photoreactor the concentration of H_2O_2 is assumed to be 50 mg/lit, the concentration of each contaminant (tributyl phosphate (TBP), tri(2-butoxyethyl) phosphate (TBEP) and tri(2-chloroethtyl) phosphate (TCEP)) is assumed to be 5 mg/lit. Also it is assumed that the wastewater at the inlet contains 25 mg/lit of the bicarbonates.

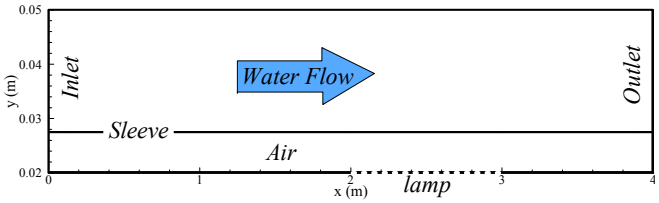

Fig. 2. Schematic view of UV-H2O2 photoreactor section

III. Results and Discussion

Fig. 3. displays the incident radiation contours obtained from 2D and 1D simulations in the UV-H_2O_2 photoreactor with radial ratio of 8. As mentioned before DO model is used in 2D simulation and MPSS model is used in 1D model. It can be seen that in both cases the UV radiation penetrates in radial direction and does not penetrate in the axial direction significantly. The incident radiation is maximum in the vicinity of the sleeve and it decreases by approaching to the outer wall of the UV-H_2O_2 photoreactor. This reduction is due to increasing of the area by increasing the radius and the absorbance of the UV beams by the water and chemical components in the water. By comparing the MPSS and DO results, it can be found that the one dimensional model (MPSS) results are less than the results obtained from DO model the incident radiation especially in the vicinity of the sleeve.

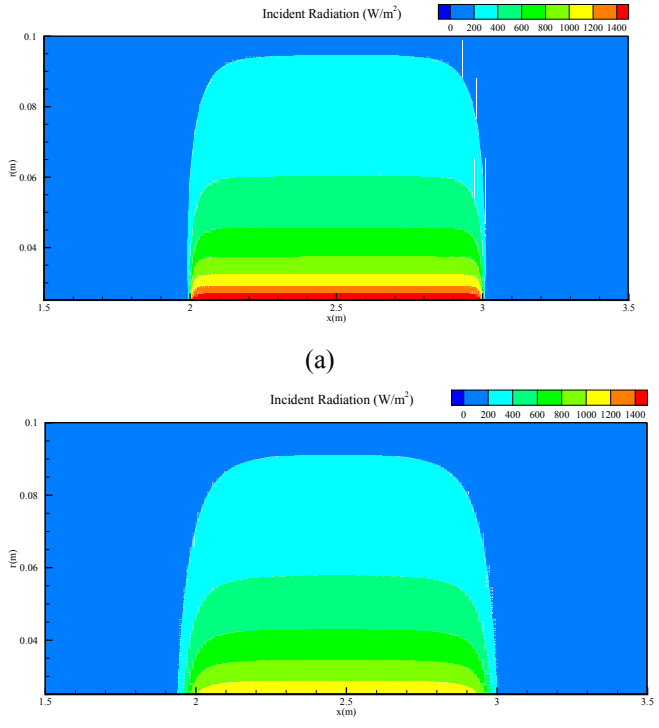

Fig. 3. Incident radiation distribution in UV-H2O2 photoreactor with radius ratio of 8 obtained from a) DO model and b) MPSS model

To compare the incident radiation results of the MPSS and DO models more precisely, the curves of the incident radiation, in three radiuses are plotted in Fig. 4. It is found that the difference of the MPSS model is greater near the sleeve and the differences between the MPSS and DO model results decreases by increasing the radius. The maximum of the discrepancies between the results is about 20 percent at r = 0.03 m.

Fig. 5 displays the curves of the H2O2 concentration obtained from one and two-dimensional simulation. It is seen that the one dimensional model greater H2O2 concentration than two dimensional model. This could be due to the fact that the MPSS model used in the one-dimensional modeling underpredict the incident radiation in the UV-H2O2 photoreactor.

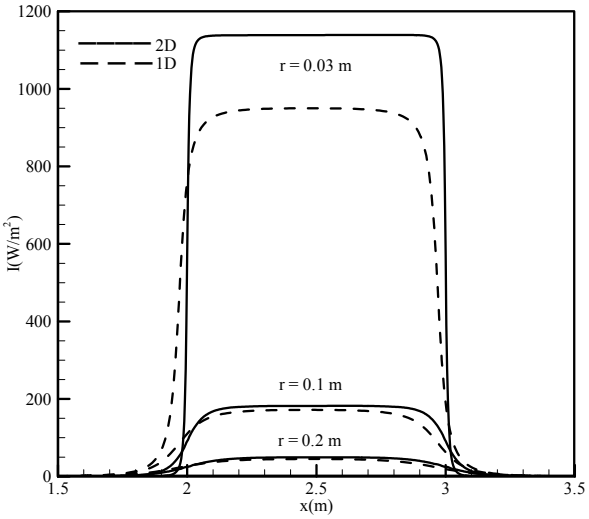

Fig. 4. Comparing the results of incident radiation curves in a constant radius in UV-H2O2 photoreactor with radial ratio of 8 obtained from DO and MPSS models.

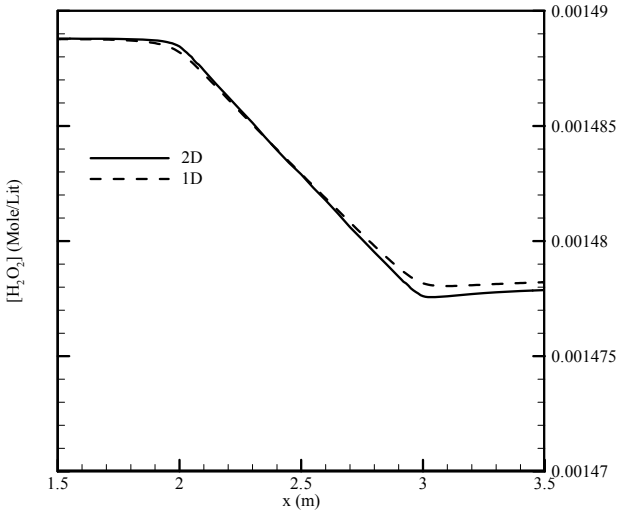

Fig. 5. Comparing H2O2 concentration along the UV-H2O2 photoreactor obtained from one and two dimensional simulation

As it is expected OH• concentration is under predicted in the 1D model. Fig. 6Fig. 6 shows that the 1D model under predicts the hydroxyl concentration about 50 percent. This is due to the smaller fluence rate in the MPSS model. Also it is consistent with the H2O2 concentrations (See Fig. 5).

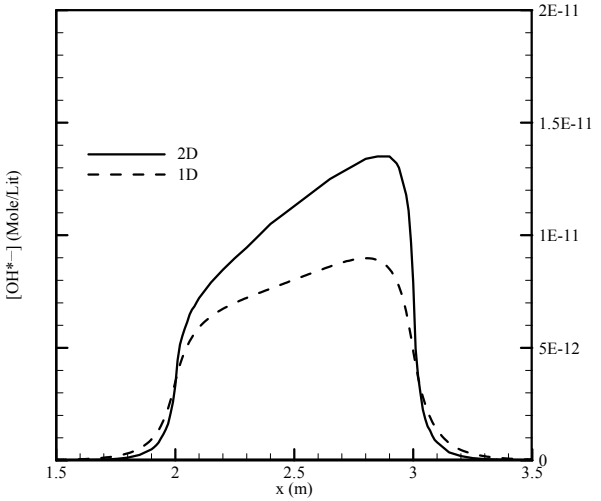

Fig. 6. Comparing OH• concentration along the UV-H2O2 photoreactor obtained from one and two dimensional simulation

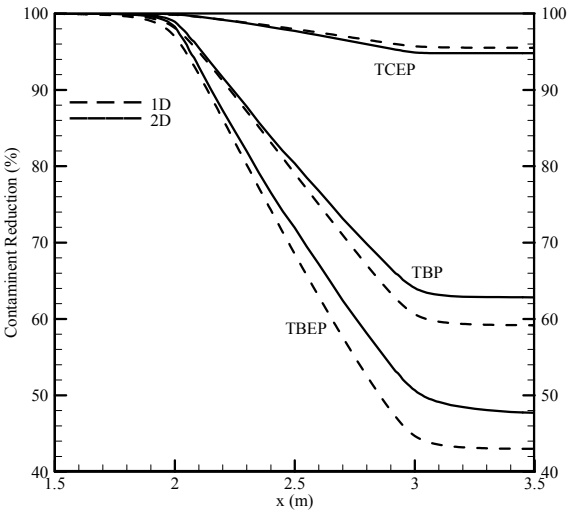

Fig. 7. Comparing contaminant concentration along the UV-H2O2 photoreactor obtained from one and two dimensional simulation

The variation of contaminant concentrations is shown in Fig. 7. It is found that the 1D model over predict the contaminant degradation. Although the 1D model under predict the hydroxyl radicals concentration, but the contaminant degradation is greater in this model, this is due to the fact that the hydroxyl radicals in 2D models are concentrated near the lamp and there is great gradients in the radial direction, but in the 1D model the hydroxyl radicals are assumed to be distributed uniformly along the radial direction and there is no radial gradient. The 1D model is the representative of fully mixed reactors that is an ideal reactor.

IV. Conclusion

In this paper, annular UV-H_2O_2 photo reactor is simulated by one and two dimensional model. It is shown that the 1D model for the UV-H_2O_2 photoreactor provide results similar to the more expensive two dimensional models. Although the hydroxyl concentration under predicted about 50 percent in the one dimensional model, removal percentage of the contaminants are consistent in both models and theaccuracy is reasonable. Obtained results show that the error of the 1D model is less than 10% for the degradation of the contaminants.

References

[1] Stefan, M. I., A. R. Hoy, and J. R. Bolton, "Kinetics and Mechanism of the Degradation and Mineralization of Acetone in Dilute Aqueous Solution Sensitized by the UV Photolysis of Hydrogen Peroxide". *Environmental Science & Technology*, 1996. 30(7): p. 2382-2390.

[2] Crittenden, J. C., S. Hu, D. W. Hand, and S. A. Green, "A kinetic model for H_2O_2/UV process in a completely mixed batch reactor". *Water Research*, 1999. 33: p. 2315-2328.

[3] Bolton, J. R., "Calculation of ultraviolet fluence rate distributions in an annular reactor: significance of refraction and reflection". *Water Research*, 2000. 34(13): p. 3315-3324.

[4] Liu, D., J. Ducoste, S. Jin, and K. Linden, "Evaluation of Alternative Fluence Rate Distribution Models". *Journal Water Supply and Research-AQUA*, 2004. 53(6): p. 391-408.

[5] Sasges, M., R., A. van der Pol, A. Voronov, and J. Robinson, "*A Standard Method for Quantifying the Output of UV Lamps"*, in *International Ozone Association Joint Congress*2007, International UV Association.

[6] Machairas, A., "*The UV/H2O2 Advanced Oxidation Process in UV Disinfection Units: Removal of Selected Phosphate Esters by Hydroxyl Radical"*, in *Department of Civil And Environmental Engineering*2004, MIT.

[7] Sozzi, D. A. and F. Taghipour, "Computational and experimental study of annular photo-reactor hydrodynamics". *International Journal of Heat and fluid flow*, 2006. 27(6): p. 1043-1053.

[8] Liu, D., C. Wu, K. Linden, and J. Ducoste, "Numerical simulation of UV disinfection reactors: Evaluation of alternative turbulence models". *Applied Mathematical Modelling*, 2007. 31(9): p. 1753-1769.

[9] Shao, L., "*Degradation of 4TBP by AOP, UV Reactor Modeling and Validation, Master Thesis"*, in *Faculty of Civil Engineering and Geosciences, Section Water Management*2007, Delft University of Technology.

[10] Hofman, J., et al., "*Design of UV reactors by CFD: Model Development and Experimental Validation"*, in *Proceedings of the COMSOL Users Conference, Grenoble*2007.

[11] Pareek, V. K., S. J. Cox, M. P. Brungs, B. Young, and A. A. Adesina, "Computational fluid dynamic (CFD) simulation of a pilot-scale annular bubble column photocatalytic reactor". *Chemical Engineering Science*, 2003. 58(3–6): p. 859-865.

[12] Santoro, D., et al., "Modeling Hydroxyl Radical Distribution and Trialkyl Phosphates Oxidation in UV−H2O2 Photoreactors Using Computational Fluid Dynamics". *Environmental Science & Technology*, 2010. 44(16): p. 6233-6241.

[13] Modest, M.F., *Radiative Heat Transfer*1993: Series in Mechanical Engineering. McGraw-Hill.